

Alma Mater Studiorum Università di Bologna  
Archivio istituzionale della ricerca

Could hypoxia influence basic biological properties and ultrastructural features of adult canine mesenchymal stem /stromal cells?

This is the final peer-reviewed author's accepted manuscript (postprint) of the following publication:

*Published Version:*

Could hypoxia influence basic biological properties and ultrastructural features of adult canine mesenchymal stem /stromal cells? / Iacono, Eleonora\*; Pascucci, Luisa; Bazzucchi, Cinzia; Cunto, Marco; Ricci, Francesca; Rossi, Barbara; Merlo, Barbara. - In: VETERINARY RESEARCH COMMUNICATIONS. - ISSN 0165-7380. - ELETTRONICO. - 42:4(2018), pp. 297-308. [10.1007/s11259-018-9738-9]

*Availability:*

This version is available at: <https://hdl.handle.net/11585/649006> since: 2019-02-12

*Published:*

DOI: <http://doi.org/10.1007/s11259-018-9738-9>

*Terms of use:*

Some rights reserved. The terms and conditions for the reuse of this version of the manuscript are specified in the publishing policy. For all terms of use and more information see the publisher's website.

This item was downloaded from IRIS Università di Bologna (<https://cris.unibo.it/>).  
When citing, please refer to the published version.

(Article begins on next page)

1

2

3

4 “This is a post-peer-review, pre-copyedit version of an article published in  
5 Veterinary Research Communications. The final authenticated version is  
6 available online at: <http://dx.doi.org/10.1007/s11259-018-9738-9>.

7

8

9

10 This version is subjected to Springer Nature terms for reuse that can be found at:  
11 <https://www.springer.com/gp/open-access/authors-rights/aam-terms-v1>

12

13

14 **Could hypoxia influence basic biological properties and ultrastructural features of adult**  
15 **canine mesenchymal stem /stromal cells?**

16

17 Eleonora Iacono<sup>1\*</sup>, 0000-0002-4435-1844

18 Luisa Pascucci<sup>2</sup>, 0000-0002-2562-1140

19 Cinzia Bazzucchi<sup>2</sup>

20 Marco Cunto<sup>1</sup>, 0000-0002-2562-1140

21 Francesca Ricci<sup>3</sup>

22 Barbara Rossi<sup>1</sup>

23 Barbara Merlo<sup>1</sup>, 0000-0001-7029-5404

24

25 <sup>1</sup>Department of Veterinary Medical Sciences, University of Bologna, Italy, via Tolara di  
26 Sopra 50, 40064, Ozzano Emilia (Bologna), Italy

27 <sup>2</sup>Department of Veterinary Medicine, University of Perugia, via San Costanzo 4, 06126,  
28 Perugia, Italy

29 <sup>3</sup>Immunohaematology and Transfusion Medicine, S.Orsola-Malpighi Hospital, Bologna, Italy

30

31 \*Corresponding to: Prof. Eleonora Iacono: <sup>1</sup>Department of Veterinary Medical Sciences,  
32 University of Bologna, Italy, via Tolara di Sopra 50, 40064, Ozzano Emilia (Bologna), Italy.

33 E-mail: [eleonora.iacono2@unibo.it](mailto:eleonora.iacono2@unibo.it).

34 Phone number: +39-0512097567.

35

36 **Acknowledgements**

37 The Authors thank Prof. Daniele Zambelli, and Dr. Giulia Ballotta, Department of Veterinary  
38 Medical Sciences, University of Bologna, for the help given in samples recovery.

39 **Abstract**

40 The aim of the present study was to compare canine adipose tissue mesenchymal stem cells  
41 cultured under normoxic (20% O<sub>2</sub>) and not severe hypoxic (7% O<sub>2</sub>) conditions in terms of  
42 marker expression, proliferation rate, differentiation potential and cell morphology. Intra-  
43 abdominal fat tissue samples were recovered from 4 dogs and cells isolated from each sample  
44 were cultured under hypoxic and normoxic conditions. Proliferation rate and adhesion ability  
45 were determined, differentiation towards chondrogenic, osteogenic and adipogenic lineages  
46 was induced; the expression of CD44, CD34, DLA-DQA1, DLA-DRA1 was determined by  
47 PCR, while flow cytometry analysis for CD90, CD105, CD45 and CD14 was carried out. The  
48 morphological study was performed by transmission electron microscopy. Canine AT-MSCs,  
49 cultured under different oxygen tensions, maintained their basic biological features. However,  
50 under hypoxia, cells were not able to form spheroid aggregates revealing a reduction of their  
51 adhesiveness. In both conditions, MSCs mainly displayed the same ultrastructural morphology  
52 and retained the ability to produce membrane vesicles. Noteworthy, MSCs cultivated under  
53 hypoxia revealed a huge shedding of large complex vesicles, containing smaller round-  
54 shaped vesicles.

55 In our study, hypoxia partially influences the basic biological properties and the  
56 ultrastructural features of canine mesenchymal stem /stromal cells. Further studies are needed  
57 to clarify how hypoxia affects EVs production in term of amount and content in order to  
58 understand its contribution in tissue regenerative mechanisms and the possible employment in  
59 clinical applications. The findings of the present work could be noteworthy for canine as well  
60 as for other mammalian species.

61 **Key words**

62 canine, mesenchymal stem cells, hypoxia, electron microscopy

63

64 **1. Introduction**

65 Naturally occurring diseases in companion animals, such as *Canis familiaris*, can be suitable  
66 models for human genetic and acquired diseases, helping to define the potential therapeutic  
67 efficiency and safety of stem cells therapy (Hayes et al., 2008; Schneider et al., 2008).

68 Furthermore, the effective management of companion animals, such as dog, for their owners  
69 requires sophisticated new treatments and preventive strategies. Mesenchymal stem/stromal  
70 cells are the most promising candidates for tissue engineering and regenerative medicine  
71 applications. To date, canine derived MSCs have been established from different tissues, such  
72 as adipose tissue (Black et al., 2007), umbilical cord (Seo et al., 2009; Zucconi et al., 2010),  
73 liver and bone marrow (Wenceslau et al., 2011). Adipose tissue is ubiquitously available and  
74 has several advantages compared to other sources, particularly to bone marrow. In fact, it is  
75 easily accessible in large quantities with minimal invasive harvesting procedures.  
76 Furthermore, adipose tissue yields a high amount of MSCs (AT-MSCs) (Schäffler and  
77 Bächler, 2007).

78 It is known that both local injection as well as systemic administration of MSCs result in the  
79 successful engraftment of a small percentage of the injected cells in the site of the injury  
80 (Chimenti et al., 2016). Consistent with these findings, some studies recently showed that the  
81 regenerative ability of MSCs could be mainly attributed to the production of molecules and  
82 mediators capable of activating the intrinsic regenerative process in the damaged tissues  
83 inhibiting apoptosis and fibrosis, enhancing angiogenesis, stimulating mitosis and/or  
84 differentiation of tissue-resident progenitor cells, and modulating the immune response  
85 (Lange-Consiglio et al., 2016). These bioactive factors are freely secreted in the extracellular  
86 environment or are enclosed in micrometric and nanometric vesicles (EVs) that are released  
87 from MSCs (Yagi et al., 2010; Liang et al., 2014). They enclose lipids, growth factors,  
88 cytokines and different kinds of RNAs that are important mediators of cell- to-cell

89 communication (Huang et al., 2013; Pascucci et al., 2014a; Pascucci et al., 2015; Crivelli et  
90 al., 2017). EVs payload and their surface markers are strictly related to cell parent lineage and  
91 are influenced by cell metabolic state during their biogenesis (Tetta et al., 2013). For these  
92 reasons, EVs have a double role in physiological and pathological conditions, equally  
93 contributing to suppress or support a pathological condition (Chaput et al., 2011), depending  
94 on whether they are “good or bad” vesicles (Lo Cicero et al., 2015). Moreover, EVs exhibit  
95 many of the superficial markers, cytokines, growth factors and the immune modulatory  
96 properties of their origin cells (Gyorgy et al., 2015). Therefore, EVs could be used as smaller  
97 cellular “alter ego”, in order to achieve innovative cell-free strategies (Gyorgy et al., 2015).  
98 Furthermore, because of their capacity to encapsulate both hydrophilic and lipophilic  
99 molecules and to deliver them, EVs from MSCs could be considered as drug delivery systems  
100 (Bonomi et al., 2017; Pascucci et al., 2014b).

101 Several Authors reported the ultrastructural features and EVs production by adult and foetal  
102 human (Budoni et al., 2013; Del Fattore et al., 2015) and equine MSCs (Pascucci et al.,  
103 2014a; Pascucci et al., 2015; Lange-Consiglio et al., 2016; Iacono et al., 2017) and their  
104 possible therapeutic applications (Budoni et al., 2013; Lange-Consiglio et al., 2016; Iacono et  
105 al., 2017). Only one study briefly described the appearance, at transmission electron  
106 microscopy, of canine bone marrow MSCs (Bonomi et al., 2017), but the EVs production by  
107 these cells was no mentioned.

108 MSCs migration towards the injured tissue increases under hypoxic conditions because low  
109 oxygen tension changes their surface receptors and the interaction with the damage tissue,  
110 even if it is strictly related to MSCs close to the injured site (Annabi et al., 2003). Moreover,  
111 AT-MSCs reside in a microenvironment with low oxygen tension (1-7%) and physiologically  
112 experiences an oxygen tension lower than the atmospheric tension (20-21%) (Choi et al.,  
113 2014; Choi et al., 2015). Both in humans and in dogs, MSCs are usually cultured at

114 atmospheric oxygen tension and the effects of hypoxia on proliferation, differentiation and  
115 molecular profiles are contradictory (Chung et al., 2012; Lee et al., 2016). No data have been  
116 reported on the effects of hypoxia on ultrastructural features and EVs production of human or  
117 animal MSCs.

118 The purpose of this study was to investigate cellular proliferation, differentiation potential,  
119 molecular profile, migration and adhesion ability under normoxia (21%) and hypoxia (7%).  
120 Moreover, we aimed at evaluating the ultrastructural features of canine AT-MSCs and their  
121 capacity to produce EVs in both culture conditions. We hypothesized that hypoxia (7%) could  
122 affect cellular metabolism and consequently the release of EVs.

123

## 124 **2. Materials and Methods**

125 Chemicals were obtained from Sigma Aldrich (St. Louis, MO, USA) and laboratory plastic  
126 ware was from Sarstedt Inc. (Newton, NC, USA) and Corning (Corning, NY, USA), unless  
127 otherwise stated.

128

### 129 *2.1 Animals*

130 Intra-abdominal fat tissue was recovered from 7 one year old bitches referred for a routine  
131 castration to the Department of Veterinary Medical Sciences, University of Bologna. The  
132 written consent was given by all owners to allow the use of removed tissue for research  
133 purposes and experimental procedures were approved by the Ethics Committee on animal use  
134 of the Department of Veterinary Medical Sciences, University of Bologna, and by the Italian  
135 Ministry of Health.

136

### 137 *2.2 Samples collection and cell isolation*

138 Immediately after removal, AT samples were stored in DPBS supplemented with antibiotics  
139 (100 IU/ml penicillin, 100 µg/ml streptomycin) and transferred to the lab. MSCs were isolated  
140 as previously described (Iacono et al., 2015). Briefly, under a laminar flow hood, tissue was  
141 rinsed by repeated immersion in DPBS, weighed and minced finely (0.5 cm) by sterile  
142 scissors. Minced AT was transferred into a 50ml polypropylene tube and a digestion solution,  
143 containing 0.1% collagenase type I (GIBCO®, ThermoFisher Scientific, Waltham,  
144 Massachusetts, USA) dissolved in DPBS, was added (1ml solution/1g tissue) mixing  
145 thoroughly. This mix was kept in a 37°C water bath for 30 min and mixed every 10 min.  
146 After incubation, collagenase was inactivated diluting 1:1 with DPBS supplemented with 10%  
147 v/v FBS (GIBCO®, ThermoFisher Scientific, Waltham, Massachusetts, USA). The resulting  
148 solution was filtered in order to discard the undigested tissue and nucleated cells were pelleted  
149 at 470 g for 10 min. The pellet was re-suspended in culture medium [DMEM: TCM199  
150 (GIBCO®, ThermoFisher Scientific, Waltham, Massachusetts, USA) = 1:1, plus 10% FBS]. It  
151 was centrifuged 3 times at 470 g for 10 min in order to rinse cells. Cell pellet was re-  
152 suspended in 1 ml of culture medium and cell concentration was evaluated by  
153 haemocytometer. For plating and culturing the same cell number under hypoxic and normoxic  
154 conditions, each sample was divided in 2 equal parts. The term “normoxic” indicates the  
155 standard culture conditions (humidified atmosphere with 5% CO<sub>2</sub> and 21% O<sub>2</sub>) while the term  
156 “hypoxic” is related to a humidified atmosphere with 5% CO<sub>2</sub> and 7% O<sub>2</sub>. Canine AT-MSCs  
157 cultured in normoxia will be indicated as Nor-AT-MSCs whereas the ones cultured under  
158 hypoxia will be indicated as Hyp-AT-MSCs.

159

### 160 *2.3 Cell culture and population doublings*

161 After isolation, primary cells derived from all recovered samples were plated in a 25 cm<sup>2</sup> flask  
162 in 5 ml of culture medium at 38.5 °C under normoxic or hypoxic conditions. After 2 days of



163 in vitro culture, the medium was completely re-placed and non-adherent cells removed.  
164 Hereafter the medium was changed twice a week until adherent primary MSCs reached ~80-  
165 90% confluence and then they were dissociated by 0.25% trypsin, counted by a  
166 haemocytometer and plated at the concentration of  $5 \times 10^3$  cells/cm<sup>2</sup> as “Passage 1” (P1).  
167 Cells were allowed to proliferate until 80-90% confluence before trypsinization and  
168 successive passage.

169 Calculation of cell-doubling time (DT) and cell-doubling numbers (CD) was carried out  
170 according to the following formulae (Rainaldi et al., 1991):

$$171 \text{ CD} = \ln(N_f / N_i) / \ln(2)$$

172 where  $N_f$  and  $N_i$  are the final and the initial number of cells, respectively;

$$173 \text{ DT} = \text{CT} / \text{CD}$$

174 where CT is the cell culture time.

175

#### 176 *2.4 Adhesion and Migration Assays*

177 To define differences between Hyp-AT-MSCs and Nor-AT-MSCs, spheroid formation and  
178 migration test were performed. For each group were carried out 3 replicates for each  
179 experiment; all replicates were carried out at passage 3 of in vitro culture.

180 For adhesion assay, cells were cultured in ‘hanging drops’ (5.000 cells/drop of 25µl) for 24 h.

181 Images were acquired by a Nikon Eclipse TE 2000-U microscope. Starting from the binary  
182 masks obtained by Image J software (Processing and Analysis in Java, Version 1.6,  
183 [imagej.nih.gov/ij/](http://imagej.nih.gov/ij/)), the volume of each spheroid was computed using ReViSP  
184 ([sourceforge.net/projects/revisp](http://sourceforge.net/projects/revisp)) (Bellotti et al., 2016), a software specifically designed to  
185 accurately estimate the volume of spheroids and to render an image of their 3D surface.

186 To assess cell migration potential, a scratch assay (also known as Wound-Healing assay) was  
187 carried out, as previously described (Liang et al., 2007). Briefly, at 80-90 % confluence the

188 cell monolayer was scraped using a p1000 pipet tip. After washing twice with DPBS, the dish  
189 was incubated for 24 h. Images were acquired both immediately after the tip-scratch (time 0;  
190 T0) and after the incubation period (last time point or time 1; T1), and the distances of each  
191 scratch closure were calculated by ImageJ software (Processing and Analysis in Java, Version  
192 1.6, [imagej.nih.gov/ij/](http://imagej.nih.gov/ij/)). The migration percentages were calculated using the following  
193 formula (Rossi et al., 2014):

$$194 \quad [(distance\ at\ T0 - distance\ at\ T1) * 100] / distance\ at\ T0$$

195

### 196 *2.5 Multilineage differentiation*

197 *In vitro* differentiation potential of cells toward osteogenic, adipogenic and chondrogenic  
198 lineages in different culture conditions was studied. Cells ( $5 \times 10^3$  cells/cm<sup>2</sup>) were cultured  
199 under specific induction media (Table 1). As negative control, an equal number of cells was  
200 cultured in expansion medium. *In vitro* differentiation potential was assessed at passage 3 of  
201 culture in two replicates for three samples from each lineage. To cytologically evaluate  
202 differentiation, cells were fixed with 10% formalin at room temperature (RT) and stained with  
203 Oil Red O, Alcian Blue and Von Kossa for adipogenic, chondrogenic and osteogenic  
204 induction, respectively. Quantitative analysis of *in vitro* differentiation was performed by  
205 ImageJ (Processing and Analysis in Java, Version 1.6, [imagej.nih.gov/ij/](http://imagej.nih.gov/ij/)).

206

### 207 *2.6 Molecular Characterization*

208 Expression of specific MSCs (CD44), hematopoietic (CD34), and major histocompatibility  
209 complex (DLA-DQA1, DLA-DRA1) markers was investigated by PCR analysis on  
210 undifferentiated Nor-AT-MSCs and Hyp-AT-MSCs (Table 2). All tests were carried out on  
211  $100 \times 10^3$  cells, derived from three different dogs. Experiments were performed at passage 3 of  
212 *in vitro* culture, except for DLA-DQA1 and DLA-DRA1: in fact, given the increasing demand  
213 of MSCs for clinical use also in the canine species, the expression of DLA-DQA1 and DLA-

214 DRA1 was also studied at P0 to assess their immunologic properties. For PCR, cells were  
215 snap-frozen and RNA was extracted using Nucleo Spin<sup>®</sup> RNA kit (Macherey-Nagel, Düren,  
216 Germany) following the manufacturer's instructions. cDNAs were synthesized by RevertAid  
217 RT Kit (ThermoFisher Scientific, Waltham, Massachusetts, USA) and used directly in PCR  
218 reactions, following the instructions of Maxima Hot Start PCR Master Mix (2X)  
219 (ThermoFisher Scientific, Waltham, Massachusetts, USA).

220 Canine glyceraldehyde-3-phosphate dehydrogenase (GAPDH) was employed as a reference  
221 gene in each sample in order to standardize the results and to assess RNA integrity and purity.  
222 Furthermore, for all primers, in order to assess sample purity, a RT- and a mix without primer  
223 were analyzed.

224 PCR products were visualized with ethidium bromide on a 2% agarose gel (Bio-Rad  
225 Laboratories, Inc., Hercules, California, USA).

226

## 227 *2.7 Flow cytometry*

228 Cytofluorimetric analysis was carried out to study the cell surface marker expression of  
229 canine Nor-AT-MSCs and Hyp-AT-MSCs. At P3 cells were labeled with CD90, CD105,  
230 CD14, and CD45 mouse monoclonal antibodies (all from Beckman Coulter, Milan, Italy) and  
231 with isotype control mouse monoclonal antibodies. Briefly, at 80-90% of confluence, cells  
232 were harvested by trypsinization after twice rinsing with DPBS and collected at a  
233 concentration of  $10^6$  cells/ml. Fixation and permeabilization were carried out using Reagent 1  
234 of Intraprep Kit (Beckman Coulter, Milan, Italy). Flow cytometry was performed using  
235 FC500 two-laser equipped cytometer (Beckman Coulter, Milan, Italy). Coniugated-specific  
236 antibodies or isotype-matched control mouse immunoglobulin G are listed in Table 3. Cross-  
237 reactivity of the antibodies used was screened using cultured human and canine MSCs.  
238 Incubated cells with isotype-specific IgGs were used as control cells in order to establish the

239 background signal. Furthermore, to verify cross-reactivity, control on circulating canine  
240 lymphocytes was carried out. The similarity of CD markers was also identified by comparing  
241 the amino acid sequences using Basic Local Alignment Search Tool (BLAST). Results were  
242 further analyzed with the CXP dedicated program.

243

#### 244 *2.8 Transmission Electron Microscopy (TEM)*

245 Ultrastructural investigation was carried out on canine Nor-AT-MSCs (n=3) and Hyp-AT-  
246 MSCs (n=3) at P3 of culture. At this time, the cells were detached from the flask by trypsin-  
247 EDTA, centrifuged at 600 g for 10 minutes to remove the medium and fixed with 2.5%  
248 glutaraldehyde in 0.1 M phosphate buffer (PB), pH 7.3, for 1 h at room temperature. They  
249 were subsequently washed twice in PB and post-fixed with 2% osmium tetroxide dissolved in  
250 0.1 M PB, pH 7.3, for 1 h at room temperature. Cells were finally dehydrated in a graded  
251 series of ethanol up to absolute, pre-infiltrated and embedded in Epon 812 (Electron  
252 Microscopy Sciences, Hatfield, Pa, USA). Ultrathin sections (90 nm) were mounted on 200-  
253 mesh copper grids, stained with uranyl acetate and lead citrate, and examined by means of a  
254 Philips EM 208, equipped with a digital camera.

255

#### 256 *2.9 Statistical analysis*

257 CDs, DTs and percentages of migration are expressed as mean  $\pm$  standard deviation.  
258 Statistical analyses were performed using IBM SPSS Statistics 23 (IBM Corporation,  
259 Armonk, New York, USA). Data were analysed, for normal distribution, using a Shapiro-  
260 Wilk test. For growth curve, DTs and CDs were analysed using Student's T Test for paired  
261 variables. To compare single culture passage DTs one-way ANOVA and post hoc Tuckey test  
262 were applied. Data recorded from scratch test were analysed by Student's T test for paired

263 variables, while the 3D spheroid volumes were compared using Wilcoxon test, due to their  
264 non-normal distribution. Significance was assessed for  $P < 0.05$ .

265

### 266 **3. Results**

267

#### 268 *3.1 Cell culture, in vitro differentiation and phenotype characterization*

269 Adherent cells with the characteristic spindle-shaped morphology were isolated from all  
270 samples and cultivated both under normoxia and hypoxia condition. For all samples, in both  
271 culture conditions, undifferentiated cells were cultured until P5. At P5, total CDs registered  
272 for Nor-AT-MSCs and Hyp-AT-MSCs were not statistically different ( $12.9 \pm 3.4$  vs  $12.7 \pm 3.2$ ;  
273  $P > 0.05$ ; Fig.1A) ( $P > 0.05$ ). No statistically significant differences ( $P > 0.05$ ) were found  
274 between total DTs in Nor-AT-MSCs and Hyp-AT-MSCs ( $3.58 \pm 2.14$  vs  $3.53 \pm 2.13$  days  
275 respectively;  $P > 0.05$ ; Fig.1B); the only difference observed was at the second passage of *in*  
276 *vitro* culture, when Nor-AT-MSCs DT ( $3.6 \pm 1.4$  days) was higher than Hyp-AT-MSCs DT  
277 ( $2.9 \pm 0.9$  days) (Fig.1B;  $P < 0.05$ ). Analysing DTs at different passage in the same culture  
278 group, both in Nor-AT-MSCs and Hyp-AT-MSCS a statistically significant increase was  
279 observed starting from P3 (Fig.1B;  $P < 0.05$ ).

280 As showed in Fig. 2A, no significant differences ( $P > 0.05$ ) in the migration abilities were  
281 observed between Nor-AT-MSCs ( $68.5 \pm 10.8$  %) and Hyp-AT-MSCs ( $76.9 \pm 10.0$ %); on the  
282 contrary, while Nor-AT-MSCs cultured in 'hanging drops' were able to form spheroids, Hyp-  
283 AT-MSCs did not form a compact spheroid (Fig.2B). For these reasons a statistically  
284 significant difference was found between spheroid volumes: the spheroid formed by Hyp-AT-  
285 MSCs was twice in volume compared to that formed by Nor-AT-MSCs ( $P < 0.05$ ).

286 In order to characterize canine Nor-AT-MSCs and Hyp-AT-MSCs, PCRs were performed for  
287 CD34 as hematopoietic marker, for CD44 as MSC marker, for dog leukocytes antigens DLA-  
288 DQA1 and DLA-DRA1. CD44 expression was detected in cells cultured under both

289 conditions, while no samples expressed CD34 (Fig.3A). DLA-DQA1 was weakly expressed  
290 only at P0, while DLA-DRA1 was not expressed by any sample, at each culture passage  
291 examined (Fig.3A).

292 Cells cultured under both atmosphere conditions resulted positive for mesenchymal markers  
293 CD90, and CD105. The haematopoietic markers CD14 and CD45 were expressed in low  
294 percentages (<20%) in all samples, with a significant difference ( $P < 0.05$ ) in the expression of  
295 CD45 between Nor-AT-MSCs and Hyp-AT-MSCs ( $8.4 \pm 1.2$  vs  $13.0 \pm 0.5$ ) (Fig.3B).

296 As well as the molecular characterization seems not to be affected by *in vitro* culture  
297 conditions, also the ability of cell to differentiate *in vitro* is similar. In fact, both Nor-AT-  
298 MSCs and Hyp-AT-MSCs, cultured in induction media were able to differentiate toward  
299 osteogenic, chondrogenic and adipogenic direction (Fig.4).

300

### 301 3.2 Transmission Electron Microscopy (TEM)

302 When analyzed by TEM, cells cultivated in both experimental conditions were characterized  
303 by a unique euchromatic nucleus with irregular profile and one or more prominent nucleoli  
304 (Figg. 5A, 6A). Cytoplasm was populated by abundant free ribosomes. Apart from some flat  
305 profiles of RER, in both cell samples the cisternal space of the RER was often greatly  
306 distended (Figg. 5C, 6B). A consistent number of mitochondria was observed in both  
307 samples. They mostly appeared elongated and were characterized by normal cristae.  
308 Membrane integrity was maintained (Figg. 5B, 6B). Golgi apparatus was well developed and  
309 typically included flattened cisternae, transport vesicles, and heterogeneous sized vacuoles,  
310 some of which were very large and filled with either electron-lucent or fine granular material  
311 (Figg. 5B, 6C). The endo-lysosomal apparatus showed a variety of appearances;  
312 multivesicular bodies (MVBs) and endo-lysosomes were quite abundant. MVBs appeared as  
313 large vacuoles more than 500 nm in diameter containing 30 to 100 nm wide intraluminal

314 small vesicles. Maturation of endosomes was reflected by the progressive increasing number  
315 of intraluminal vesicles. Endo-lysosomes, on the other hand, appeared as vacuolar structures  
316 characterized by nano-vesicles, typical of late endosomes, mixed with aggregates of electron-  
317 dense material and occasional para-crystalline formations. Endo-lysosomes were present in  
318 both cell types, but they were more abundant in cells cultured under hypoxia (Figg. 5C, 5D,  
319 6B). Autophagic vacuoles were occasionally seen in Hyp-AT-MSCs. Cellular membrane  
320 showed an irregular profile due to the presence of cytoplasmic pseudopodial evaginations and  
321 to the occurrence of large complex vesicles shedding from the cell surface. This latter  
322 phenomenon appeared more evident in Hyp-AT-MSCs where large electron-lucent vesicles  
323 frequently budded from the cell surface. These vesicles were 2000 nm or even larger in  
324 diameter and contained round-shaped 300 to 500 nm wide vesicles inside their lumen (Figg.  
325 5F, 6E, 6F). Under both atmospheric conditions the extracellular space was populated by  
326 numerous vesicles of heterogeneous size (Figg. 5E, 6D).

327

#### 328 **4. Discussion**

329 The use of MSCs for regenerative medicine has been proposed in human and veterinary  
330 species (Fortier and Travis, 2011). The most studied source of MSCs is bone marrow; in  
331 particular, some Authors suggested that it may be a superior source of MSCs for osteogenesis  
332 since, in this microenvironment, cells are pre-committed towards the osteogenic lineage (Noël  
333 et al., 2008). Adipose tissue is another ideal source of MSCs: it is abundant and can be easily  
334 obtained from several body's regions with minimal side effects for donor (Tapp et al., 2009).  
335 Initially, the beneficial effect of MSCs was thought to derive from their proliferation and  
336 differentiation (Kopen et al., 1999). However, the observation that only a small number of  
337 transplanted cells survive and integrate into host damaged tissue has highlighted the  
338 possibility that an alternative mechanism exists. Today, it is widespread opinion that MSCs

339 create optimal environmental conditions for tissue regeneration via a paracrine mechanism  
340 (Pascucci et al., 2014a; Crivelli et al., 2017). In particular, MSCs produce trophic factors,  
341 cytokines and signaling molecules, able to influence angiogenesis, cell proliferation,  
342 apoptosis and even recruitment of resident stem cells (Pascucci et al., 2014a). The complex  
343 interaction between MSCs and tissue microenvironment might involve both soluble factors  
344 and production of extracellular vesicles containing various molecules (György et al., 2011).  
345 The importance of tissue environmental factors, like oxygen tension, has been previously  
346 studied in human MSCs in relation to differentiation capability (Cicione et al., 2013) and cell  
347 growth (Hung et al., 2012). *In vitro*, cell cultures are generally carried out under 20-21% O<sub>2</sub>,  
348 known as normoxia, but it does not replicate the physiological or pathological hypoxia  
349 corporeal conditions (He et al., 2007). For this reason, recently many research groups have  
350 been started to compare culture and differentiation of MSCs in normoxia and hypoxia (5%  
351 O<sub>2</sub>) or severe hypoxia (1-3% O<sub>2</sub>) (Buravkova et al., 2014). Results obtained in the present  
352 study are similar to those reported previously by Chung et al. (2012) about canine AT-MSCs  
353 growth rate in normoxia (21%) and in hypoxia (7%), but different from those reported by  
354 other Authors (Lee et al., 2016). This confirms, as already reported in humans, the disparity in  
355 results obtained culturing cells under hypoxic conditions (Choi et al., 2017). Because the  
356 effects of hypoxia on proliferation rate of AT-MSCs could be influenced not only by oxygen  
357 rate but also by other different factors, such as area of body from which it was removed,  
358 different sexes and age of donor, further studies are needed to verify if this could be true also  
359 in canine species.

360 Beyond the growth curve, migration ability is an important feature of MSCs because of its  
361 fundamental significance for systemic application (Li et al., 2009; Burk et al., 2013). No  
362 differences were found between Nor-AT-MSCs and Hyp-AT-MSCs in migration ability.  
363 Since the adhesion capability is related and enhanced to differentiation potential (Pasquinelli



364 et al., 2007; Wang et al., 2009), in the present study, for the first time in canine species,  
365 spheroid formation *in vitro* was assessed using the hanging drop method. Cells cultured under  
366 normoxia showed a higher adhesion ability, forming smaller spheroids. However, no  
367 difference were observed in differentiation ability of cells cultured in induction medium in  
368 21% and 7% O<sub>2</sub>. This could be related to the further reduction of oxygen within the  
369 micromasses which therefore requires a further adaptation of the cells to the new condition.

370 As previously reported (Chung et al., 2012; Lee et al., 2016), also under our culture  
371 conditions canine AT-MSCs maintain their stemness and the characteristic molecular profile.  
372 In fact, both Nor and Hyp-AT-MSCs expressed CD44 and did not express CD34, a  
373 hematopoietic marker. Furthermore, by RT-PCR, we demonstrated that, at P3 of *in vitro*  
374 culture in normoxia and hypoxia, canine AT-MSCs did not express DLA-DRA1 and DLA-  
375 DQA1. Furthermore, as previously reported in canine MSCs (Seo et al., 2009; Filioli Uranio  
376 et al., 2014), we found a very weak expression of DLA-DRA1 at P0. We could postulate that  
377 the expression of these markers has been lost during the first passages in canine AT-MSCs,  
378 confirming the low immunogenicity of these populations of cells and supporting their possible  
379 use for allo- and xenotransplantation.

380 With the exception of a few reports, MSCs morphology has been widely disregarded in the  
381 past years (Budoni et al., 2013; Pascucci et al., 2014a; Del Fattore et al., 2015; Pascucci et al.,  
382 2015; Lange-Consiglio et al., 2016; Iacono et al., 2017). In this manuscript, we discussed the  
383 establishment of MSCs cultures from canine adipose tissue and described, for the first time,  
384 their fine structure by transmission electron microscopy. Furthermore, since also in canine  
385 species it was demonstrated that oxygen concentration is an important component of stem cell  
386 niche (Chung et al., 2012; Lee et al., 2016) but no data are present on the effects of oxygen  
387 tension on cellular components and their ability to produce EVs, we ascertained, by means of  
388 electron microscopy, that canine AT-MSCs constitutively produce EVs under different

389 oxygen tensions and we compared the effect of normoxia (21%) and hypoxia (7%) on canine  
390 AT-MSCs fine structure. The ultrastructural morphology was mainly maintained in Hyp-AT-  
391 MSCs when compared with Nor-AT-MSCs. Canine AT-MSCs were homogeneous in shape  
392 and dimensions and presented a large, irregular nucleus with multiple nucleoli, as a sign of  
393 intense metabolic activity. This was confirmed by a consistent number of mitochondria. The  
394 main differences between Hyp-AT-MSCs and Nor-AT-MSCs attained the presence of  
395 occasional autophagosomes, the increased number of endolysosomes and the abundance of  
396 large complex vesicles budding from the cell surface and containing smaller vesicles in cells  
397 cultured in 7% O<sub>2</sub>. This particular kind of EVs has never been described before in the  
398 literature in dogs, but it was frequently observed by the authors in MSCs of different species  
399 and tissue sources (Pascucci et al., 2014a; Pascucci et al., 2015). Concerning endolysosomes  
400 and autophagosomes, it could be hypothesized that the hypoxic environment could induce a  
401 mild injury because of the reduced oxygen availability, followed by the digestion of damaged  
402 cell components. Therefore, autophagy may be interpreted as a reactive behavior of the cell to  
403 the adverse environmental conditions. The increased number of large complex vesicles  
404 budding from the cell surface and containing smaller vesicles, and the great quantity of MVBs  
405 and extracellular vesicles led to hypothesize that the high metabolic and synthetic activity  
406 typical of MSCs is enhanced in Hyp-AT-MSCs respect to cells cultured in normoxia. This is  
407 supported by the presence of an unchanged synthetic apparatus formed by the euchromatic  
408 nucleus, by a great number of free ribosomes, by a well developed RER and Golgi apparatus.  
409 This last one, additionally, produce large vacuoles containing a fine granular material that  
410 could be addressed to secretion. Examination of cell monolayers by TEM, allowed to  
411 hypothesize that EVs production could be influenced by the *in vitro* culture oxygen tension.  
412 Particularly, we observed that in cells cultured under low oxygen tension, large complex EVs  
413 seems to be more numerous. As previously speculated (Pascucci et al., 2015), it is possible

414 that this kind of vesicles encloses smaller vesicles that, in a first phase, are grouped in specific  
415 areas, underneath the plasma membrane and are then exocytosed through an apocrine-like  
416 secretion. In this way, cells are able to package a large amount of cargo enclosed inside large  
417 complex vesicles. Even if their content needs still to be characterized, it could be speculated  
418 that it may be able to modulate, at the same time, different biological pathways so inducing a  
419 strong and polymorfous environmental response.

420 In equine species, it was recently demonstrated that AT-MSCs EVs are involved in  
421 modulation of different stages of angiogenesis (Pascucci et al., 2014a). Different Authors  
422 stated that hypoxia increases the secretion of angiogenic factors and that the medium  
423 conditioned by hypoxic-treated cells may enhance angiogenesis and perfusion in nude mice  
424 with ischemic hindlimbs (Rehman et al., 2004; Stubbs et al., 2012). Furthermore, hypoxic-  
425 treated cells were found to increase secretion of antitapoptotic factors, such as IL-6: this factor  
426 has been demonstrated to inhibit cardiomyocyte apoptosis and reduce infarct size (Matsushita  
427 et al., 2005; Jung et al., 2009; Przybyt et al., 2013). Recently, it was demonstrated that canine  
428 bone marrow MSCs loaded with paclitaxel (PTX) are able to release it affecting in vitro  
429 cancer cells proliferation (Bonomi et al., 2017). PTX release could be partly mediated by  
430 EVs, as previously demonstrated in an in vitro murine model. Considering that tumor  
431 environment is often characteristically hypoxic, the possible therapeutic use of MSC  
432 cultivated under hypoxia to produce EVs to be used as drug delivery system deserves a  
433 careful further study also in canine species.

434 The results of the present study indicate that MSCs from canine adipose tissue constitutively  
435 produce EVs that may be responsible of their paracrine activity. Furthermore, the EVs  
436 production seems to be influenced by *in vitro* culture oxygen tension. There is need for further  
437 mechanistic studies of hypoxia to elucidate its influence not only on EVs production but also  
438 in their composition in view of clinical and pharmaceutical applications.

439

440 **5. Author's declaration of interest:** No competing interests have been declared.

441

442

443

444       **6. References**

- 445 Annabi B, Lee YT, Turcotte S, Naud E, Desrosiers RR, Champagne M, Eliopoulos N,  
446 Galipeau J, Béliveau R (2003) Hypoxia promotes murine bone-marrow-derived stromal cell  
447 migration and tube formation. *Stem Cells* 21:337-347. [https://doi.org/10.1634/stemcells.21-3-](https://doi.org/10.1634/stemcells.21-3-337)  
448 337.
- 449 Bellotti C, Duchi S, Bevilacqua A, Lucarelli E, Piccinini F (2016) Long term morphological  
450 characterization of mesenchymal stromal cells 3D spheroids built with a rapid method based  
451 on entry-level equipment. *Cytotechnology* 68:2479-2490. [https://doi.org/ 10.1007/s10616-](https://doi.org/10.1007/s10616-016-9969-y)  
452 016-9969-y.
- 453 Black LL, Gaynor J, Gahring D, Adams C, Aron D, Harman S, Gungerich DA, Harman R  
454 (2007) Effect of adipose-derived mesenchymal stem and regenerative cells on lameness in  
455 dogs with chronic osteoarthritis of the coxofemoral joints: a randomized, double-blinded,  
456 multi- center, controlled trial. *Vet Ther* 8:272-284.
- 457 Bonomi A, Ghezzi E, Pascucci L, Aralla M, Ceserani V, Pettinari L, Coccè V, Guercio A,  
458 Alessandri G, Parati E, Brini AT, Zeira O, Pessina A (2017) Effect of canine mesenchymal  
459 stromal cells loaded with paclitaxel on growth of canine glioma and human glioblastoma cell  
460 lines. *Vet J* 223:41-47. <https://doi.org/10.1016/j.tvjl.2017.05.005>.
- 461 Budoni M, Fierabracci A, Luciano R, Petrini S, Di Ciommo V, Muraca M (2013) The  
462 immunosuppressive effect of mesenchymal stromal cells on B lymphocytes is mediated by  
463 membrane vesicles. *Cell Transplant* 22:369-379. <https://doi.org/10.3727/096368911X582769>.
- 464 Buravkova LB, Andreeva ER, Gogvadze V, Zhivotovsky B (2014) Mesenchymal stem cells  
465 and hypoxia: Where are we? *Mitochondrion* 19PtA:105-112.  
466 <https://doi.org/10.1016/j.mito.2014.07.005>.

467 Burk J, Ribitsch I, Gittel C, Juelke H, Kasper C, Staszyc C, Brehm W (2013) Growth and  
468 differentiation characteristics of equine mesenchymal stromal cells derived from different  
469 sources. *Vet J* 195:98-106. <https://doi.org/10.1016/j.tvjl.2012.06.004>.

470 Chaput N, They C (2011) Exosomes: immune properties and potential clinical  
471 implementations. *Semin Immunopathol* 33:419-440. [https://doi.org/10.1007/s00281-010-](https://doi.org/10.1007/s00281-010-0233-9)  
472 0233-9.

473 Chimenti I, Smith RR, Li TS, Gerstenblith G, Messina E, Giacomello A, Marbán E (2016)  
474 Relative roles of direct regeneration versus paracrine effects of human cardiosphere-derived  
475 cells transplanted into infarcted mice. *Circ Res* 106:971-980.  
476 <https://doi.org/10.1161/CIRCRESAHA.109.210682>.

477 Choi JR, Pinguan-Murphy B, Wan Abas WA, Yong KW, Poon CT, Noor Azmi MA, Omar  
478 SZ, Chua KH, Wan Safwani WK (2014) Impact of low oxygen tension on stemness,  
479 proliferation and differentiation potential of human adipose-derived stem cells., *Biochem*  
480 *Biophys Res Commun* 448:218-224. <https://doi.org/10.1016/j.bbrc.2014.04.096>.

481 Choi JR, Pinguan-Murphy B, Wan Abas WA, Yong KW, Poon CT, Noor Azmi MA, Omar  
482 SZ, Chua KH, Xu F, Wan Safwani WK (2015) In situ normoxia enhances survival and  
483 proliferation rate of human adipose tissue-derived stromal cells without increasing the risk of  
484 tumour genesis. *PLoS One* 10:e0115034. <https://doi.org/10.1371/journal.pone.0115034>

485 Choi JR, Yong KW, Wan Safwani WKZ (2017) Effect of hypoxia on human adipose-  
486 derived mesenchymal stem cells and its potential clinical applications. *Cell Mol Life Sci*  
487 74:2587-2600. <https://doi.org/10.1007/s00018-017-2484-2>

488 Chung DA, Hayashi K, Chrisoula A, Toupadakis CA, Wong A, Yellowley CE (2012)  
489 Osteogenic proliferation and differentiation of canine bone marrow and adipose tissue derived  
490 mesenchymal stromal cells and the influence of hypoxia. *Res Vet Sci* 92:66-75.  
491 <https://doi.org/10.1016/j.rvsc.2010.10.012>.

492 Cicione C, Muiños-López E, Hermida-Gómez T, Fuentes-Boquete I, Díaz-Prado S, Blanco FJ  
493 (2013) Effects of severe hypoxia on bone marrow mesenchymal stem cells differentiation  
494 potential. *Stem Cells Int*:232896. <http://dx.doi.org/10.1155/2013/232896>.

495 Crivelli B, Chlapanidas T, Perteghella S, Lucarelli E, Pascucci L, Brini AT, Ferrero I,  
496 Marazzi M, Pessina A, Torre ML (2017) Mesenchymal stem/stromal cell extracellular  
497 vesicles: From active principle to next generation drug delivery system. *J Control Release*  
498 262:104-117. <https://doi.org/10.1016/j.jconrel.2017.07.023>.

499 Del Fattore A, Luciano R, Pascucci L, Goffredo BM, Giorda E, Scapatucci M, Fierabracci A,  
500 Muraca M (2015) Immunoregulatory effects of mesenchymal stem cell-derived extracellular  
501 vesicles on T lymphocytes. *Cell Transplant* 24:2615-2627.  
502 <https://doi.org/10.3727/096368915X687543>.

503 Filioli Uranio M, Dell'Aquila ME, Caira M, Guaricci AC, Ventura M, Catacchio CR, Ventura  
504 M, Cremonesi F (2014) Characterization and in vitro differentiation potency of early-passage  
505 canine amnion- and umbilical cord-derived mesenchymal stem cells as related to gestational  
506 age. *Mol Reprod Dev* 81:539-551. <https://doi.org/10.1002/mrd.21311>.

507 Fortier LA, Travis AJ (2011) Stem cells in veterinary medicine. *Stem Cell Res Ther* 2:9.  
508 <https://doi.org/10.1186/scrt50>

509 Gyorgy B, Hung ME, Breakefield XO (2015) Therapeutic applications of extracellular  
510 vesicles: clinical promise and open questions. *Ann Rev Pharmacol Toxicol* 55:439-464.

511 Hayes B, Fagerlie SR, Ramakrishnan A, Baran S, Harkey M, Graf L, Bar M, Bendoraite A,  
512 Tewari M, Torok-Storb B (2008) Derivation, characterization, and in vitro differentiation of  
513 canine embryonic stem cells. *Stem Cells* 26:465-473. <https://doi.org/10.1634/stemcells.2007->  
514 0640.

515 He MC, Li J, Zhao CH (2007) Effect of hypoxia on mesenchymal stem cells - review. *J Exp*  
516 *Hematol Chinese Ass Pathophys* 15:433-436.

517 Huang YC, Parolini O, Deng L (2013) The potential role of microvesicles in mesenchymal  
518 stem cell-based therapy. *Stem Cells Dev* 15:841-844. <https://doi.org/10.1089/scd.2012.0631>.

519 Hung SP, Ho JH, Shih YR, Lo T, Lee OK (2012) Hypoxia promotes proliferation and  
520 osteogenic differentiation potentials of human mesenchymal stem cells. *J Orthop Res* 30:260-  
521 266. <https://doi.org/10.1002/jor.21517>.

522 Iacono E, Merlo B, Romagnoli N, Rossi B, Ricci F, Spadari A (2015) Equine Bone Marrow  
523 and Adipose Tissue Mesenchymal Stem Cells: Cytofluorimetric Characterization, In Vitro  
524 Differentiation, and Clinical Application. *J Eq Vet Sci* 35:130-140.  
525 <https://doi.org/10.1016/j.jevs.2014.12.010>.

526 Iacono E, Pascucci L, Rossi B, Bazzucchi C, Lanci A, Ceccoli M, Merlo B (2017)  
527 Ultrastructural characteristics and immune profile of equine MSCs from fetal adnexa.  
528 *Reproduction* 154:509-519. <https://doi.org/10.1530/REP-17-0032>.

529 Jung DI, Ha J, Kang BT, Kim JW, Quan FS, Lee JH, Woo EJ, Park HM (2009) A comparison  
530 of autologous and allogenic bone marrow-derived mesenchymal stem cell transplantation in  
531 canine spinal cord injury. *J Neurol Sci* 285:67-77. <https://doi.org/10.1016/j.jns.2009.05.027>.

532 Kopen GC, Prockop DJ, Phinney DG (1999) Marrow stromal cells migrate throughout  
533 forebrain and cerebellum, and they differentiate into astrocytes after injection into neonatal  
534 mouse brains. *Proc Nat Acad Sci U S A* 96:10711-10716.  
535 <https://doi.org/10.1073/pnas.96.19.10711>.

536 Lange-Consiglio A, Perrini C, Tasquier R, Deregibus MC, Camussi G, Pascucci L, Marini  
537 MG, Corradetti B, Bizzaro D, De Vita B, Romele P, Parolini O, Cremonesi F (2016) Equine  
538 Amniotic Microvesicles and Their Anti-Inflammatory Potential in a Tenocyte Model In Vitro.  
539 *Stem Cells Dev* 25:610-621. <https://doi.org/10.1089/scd.2015.0348>.



540 Lee J, Byeon JS, Lee KS, Gu NY, Lee GB, Kim HR, Cho IS, Cha SH (2016) Chondrogenic  
541 potential and anti-senescence effect of hypoxia on canine adipose mesenchymal stem cells.  
542 *Vet Res Commun* 40:1-10. <https://doi.org/10.1007/s11259-015-9647-0>.

543 Li G, Zhang X, Wang H, Wang X, Meng CL, Chan CY, Yew DT, Tsang KS, Li K, Tsai SN,  
544 Ngai SM, Han ZC, Lin MC, He ML, Kung HF (2009) Comparative proteomic analysis of  
545 mesenchymal stem cells derived from human bone marrow, umbilical cord and placenta:  
546 implication in the migration. *Proteomics* 9:20-30. <https://doi.org/10.1002/pmic.200701195>.

547 Liang CC, Park AY, Guan JL (2007) In vitro scratch assay: a convenient and inexpensive  
548 method for analysis of cell migration in vitro. *Nat Protoc* 2:329-333.  
549 <https://doi.org/10.1038/nprot.2007.30>.

550 Liang X, Ding Y, Zhang Y, Tse FT, Lian Q (2014) Paracrine mechanisms of mesenchymal  
551 stem cell-based therapy: current status and perspectives. *Cell Transplant* 23:1045-1059.  
552 <https://doi.org/10.3727/096368913X667709>.

553 Lo Cicero A, Stahl PD, Raposo G (2015) Extracellular vesicles shuffling intercellular  
554 messages: for good or for bad. *Curr Opin Cell Biol* 35:69-77.  
555 <https://doi.org/10.1016/j.ceb.2015.04.013>.

556 Matsushita K, Iwanaga S, Oda T, Kimura K, Shimada M, Sano M, Umezawa A, Hata J,  
557 Ogawa S (2005) Interleukin-6/soluble interleukin-6 receptor complex reduces infarct size via  
558 inhibiting myocardial apoptosis. *Lab Invest* 85:1210-1223.  
559 <https://doi.org/10.1038/labinvest.3700322>.

560 Noël D, Caton D, Roche S, Bony C, Lehmann S, Casteilla L, Jorgensen C, Cousin B (2008)  
561 Cell specific differences between human adipose-derived and mesenchymal-stromal cells  
562 despite similar differentiation potentials. *Exp Cell Res* 314:1575-1584.  
563 <https://doi.org/10.1016/j.yexcr.2007.12.022>.

564 Pascucci L, Alessandri G, Dall'Aglio C, Mercati F, Coliolo P, Bazzucchi C, Dante S, Petrini  
565 S, Curina G, Ceccarelli P (2014a) Membrane vesicles mediate pro-angiogenic activity of  
566 equine adipose-derived mesenchymal stromal cells. *Vet J* 202:361-366.  
567 <https://doi.org/10.1016/j.tvjl.2014.08.021>.

568 Pascucci L, Coccè V, Bonomi A, Ami D, Ceccarelli P, Ciusani E, Viganò L, Locatelli A,  
569 Sisto F, Doglia SM, Parati E, Bernardo ME, Muraca M, Alessandri G, Bondiolotti G, Pessina  
570 A (2014b) Paclitaxel is incorporated by mesenchymal stromal cells and released in exosomes  
571 that inhibit in vitro tumor growth: a new approach for drug delivery. *J Control Release*  
572 192:262-270. <https://doi.org/10.1016/j.jconrel.2014.07.042>.

573 Pascucci L, Dall'Aglio C, Bazzucchi C, Mercati F, Mancini MG, Pessina A, Alessandri G,  
574 Giammarioli M, Dante S, Brunati G, Ceccarelli P (2015) Horse adipose-derived mesenchymal  
575 stromal cells constitutively produce membrane vesicles: a morphological study. *Histol*  
576 *Histopathol* 30:549-557. <https://doi.org/10.14670/HH-30.549>.

577 Pasquinelli G, Tazzari PL, Ricci F, Vaselli C, Buzzi M, Conte R, Orrico C, Foroni L, Stella  
578 A, Alviano F, Bagnara GP, Lucarelli (2007) Ultrastructural characteristics of human  
579 mesenchymal stromal (stem) cells derived from bone marrow and term placenta. *Ultrastr*  
580 *Pathol* 31:23-31. <https://doi.org/10.1080/01913120601169477>.

581 Przybyt E, Krenning G, Brinker MG, Harmsen MC (2013) Adipose stromal cells primed with  
582 hypoxia and inflammation enhance cardiomyocyte proliferation rate in vitro through STAT3  
583 and Erk1/2. *J Transl Med* 11:39. <https://doi.org/10.1186/1479-5876-11-39>.

584 Rainaldi G, Pinto B, Piras A, Vatteroni L, Simi S, Citti L (1991) Reduction of proliferative  
585 heterogeneity of CHEF18 Chinese hamster cell line during the progression toward  
586 tumorigenicity. *In Vitro Cell Dev Biol* 27:949-952.

587 Rehman J, Traktuev D, Li J, Temm-Grove CJ, Bovenkerk JE, Pell CL, Johnstone BH,  
588 Considine RV, March KL (2004) Secretion of angiogenic and antiapoptotic factors by human

589 adipose stromal cells. *Circulation* 109:1292-1298.  
590 <https://doi.org/10.1161/01.CIR.0000121425.42966.F1>.

591 Rossi B, Merlo B, Colleoni S, Iacono E, Tazzari PL, Ricci F, Lazzari G, Galli C (2014).  
592 Isolation and in vitro characterization of bovine amniotic fluid derived stem cells at different  
593 trimesters of pregnancy. *Stem Cell Rev* 10:712-724. <https://doi.org/10.1007/s12015-014->  
594 9525-0.

595 Schäffler A, Büchler C (2007) Concise review: adipose tissue-derived stromal cells - basic  
596 and clinical implications for novel cell-based therapies. *Stem Cells* 25:818-827.  
597 <https://doi.org/10.1634/stemcells.2006-0589>.

598 Schneider MR, Wolf E, Braun J, Kolb HJ, Adler H (2008) Canine embryo-derived stem cells  
599 and models for human diseases. *Hum Mol Genet* 17: R42-47.  
600 <https://doi.org/10.1093/hmg/ddn078>.

601 Seo MS, Jeong YH, Park JR, Park SB, Rho KH, Kim HS, Yu KR, Lee SH, Jung JW, Lee YS,  
602 Kang KS (2009) Isolation and characterization of canine umbilical cord blood-derived  
603 mesenchymal stem cells. *J Vet Sci* 10:181-187. <https://doi.org/10.4142/jvs.2009.10.3.181>.

604 Stubbs SL, Hsiao ST, Peshavariya HM, Lim SY, Disting GJ, Dilley RJ (2012) Hypoxic  
605 preconditioning enhances survival of human adipose-derived stem cells and conditions  
606 endothelial cells in vitro. *Stem Cells Dev* 21:1887-1896.  
607 <https://doi.org/10.1089/scd.2011.0289>.

608 Tapp H, Hanley EN Jr, Patt JC, Gruber HE (2009) Adipose-derived stem cells:  
609 characterization and current application in orthopaedic tissue repair. *Exp Biol Med* 234:1-9.  
610 <https://doi.org/10.3181/0805/MR-170>.

611 Tetta C, Ghigo E, Silengo L, Deregibus MC, Camussi G (2013) Extracellular vesicles as an  
612 emerging mechanism of cell-to-cell communication. *Endocrine* 44:11-19.  
613 <https://doi.org/10.1007/s12020-012-9839-0>.

614 Wang W, Itaka K, Ohba S, Nishiyama N, Chung UI, Yamasaki Y, Kataoka K (2009) 3D  
615 spheroid culture system on micropatterned substrates for improved differentiation efficiency  
616 of multipotent mesenchymal stem cells. *Biomaterials* 30:2705-2715.  
617 <https://doi.org/10.1016/j.biomaterials.2009.01.030>

618 Wenceslau CV, Miglino MA, Martins DS, Ambrosio CE, Lizier NF, Pignatari GC, Kerkis I  
619 (2011) Mesenchymal progenitor cells from canine fetal tissues: yolk sac, liver, and bone  
620 marrow. *Tissue Eng Part A* 17:2165-2176. <https://doi.org/10.1089/ten.tea.2010.0678>.

621 Yagi H, Soto-Gutierrez A, Parekkadan B, Kitagawa Y, Tompkins RG, Kobayashi N,  
622 Yarmush ML (2010) Mesenchymal stem cells: mechanisms of immunomodulation and  
623 homing. *Cell Transplant* 19:667-679. <https://doi.org/10.3727/096368910X508762>.

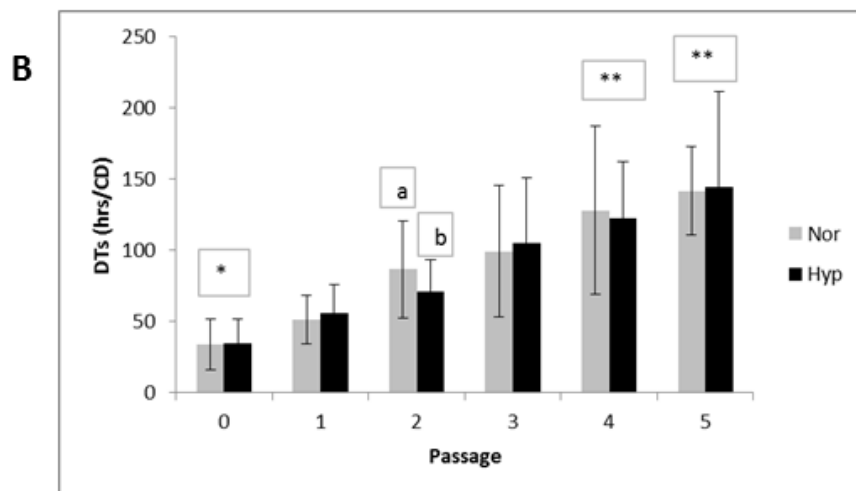
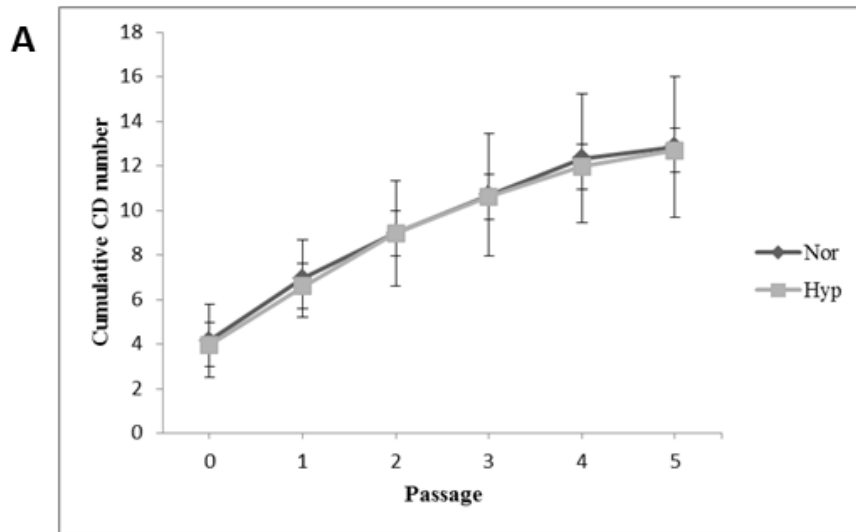
624 Zucconi E, Vieira NM, Bueno DF, Secco M, Jazedje T, Ambrosio CE, Passos-Bueno MR,  
625 Miglino MA, Zatz M (2010) Mesenchymal stem cells derived from canine umbilical cord  
626 vein-A novel source for cell therapy studies. *Stem Cells Dev* 19:395-402.  
627 <https://doi.org/10.1089/scd.2008.0314>.

628

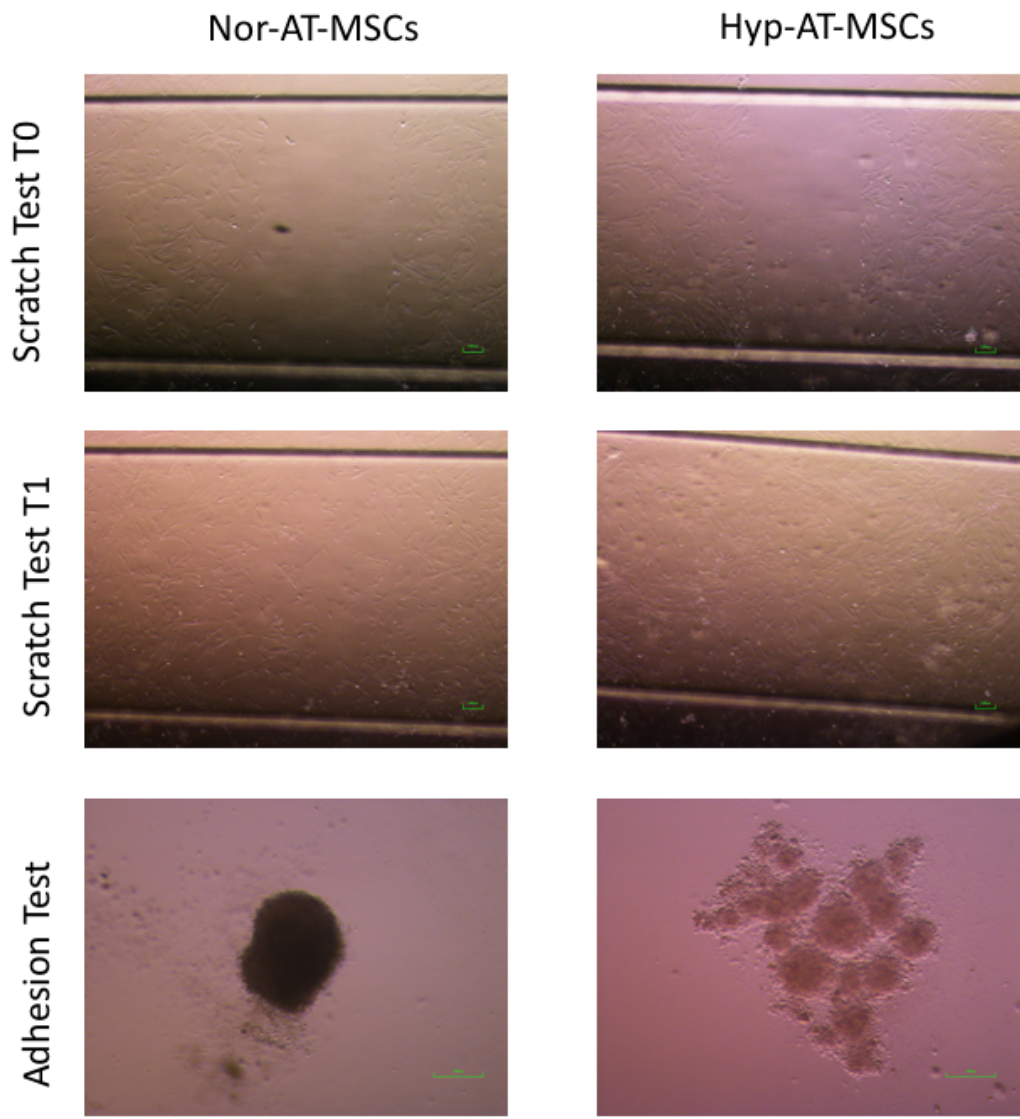
629 **Figure legends:**

630 **Fig. 1.** Total Cell Doublings (A) and Doubling times (B) of Nor-AT-MSCs and Hyp-AT-

631 MSCs over five passages of culture. A vs b, and \* vs \*\*:  $P < 0.05$ .

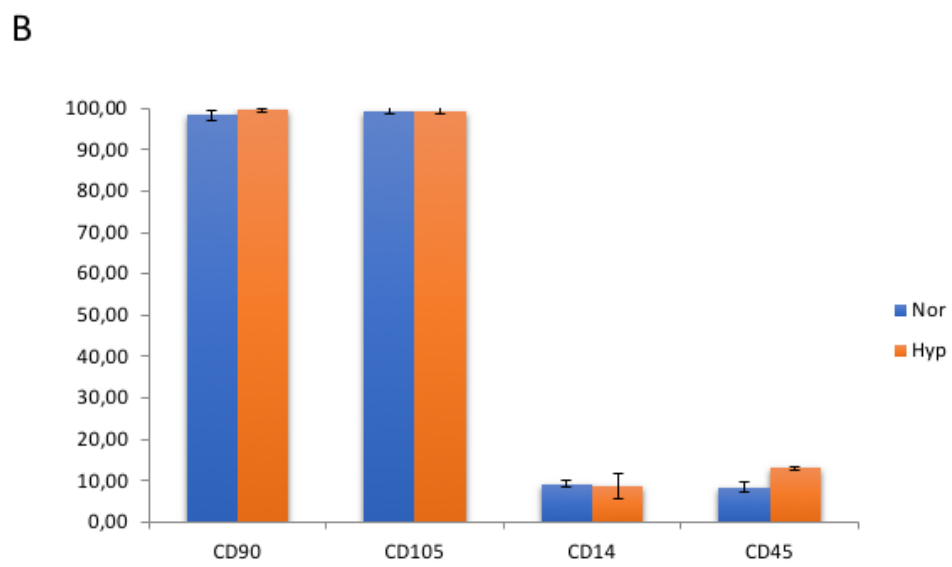
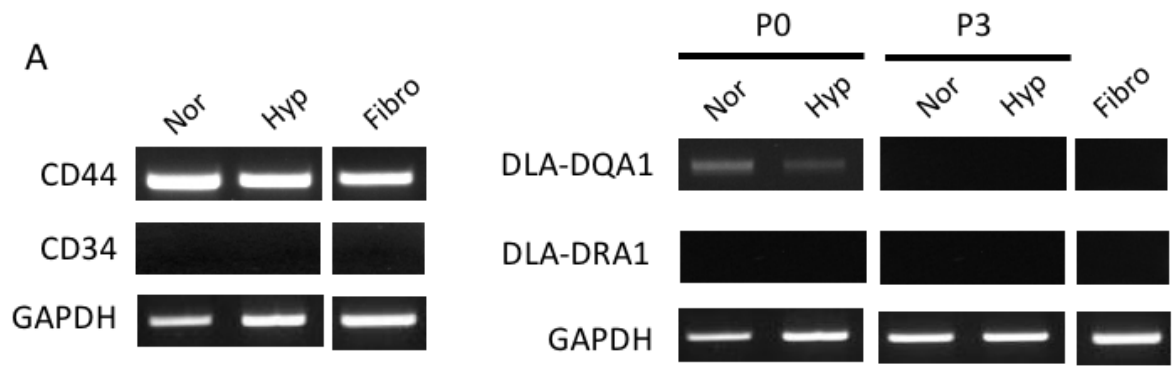


633 **Fig. 2.** A: Scratch assay on Nor-AT-MSCs and Hyp-AT-MSCs at T0 and after 24 h (T1) of  
634 cell growth (Magnification 4X, scale bar 100  $\mu\text{m}$ ). B: Adhesion assay: Volume reconstruction  
635 and visualization of a Nor- and Hyp-AT-MSC spheroid, obtained after 48 h of hanging drop  
636 culture (Magnification 10x, scale bar 10 $\mu\text{m}$ ).

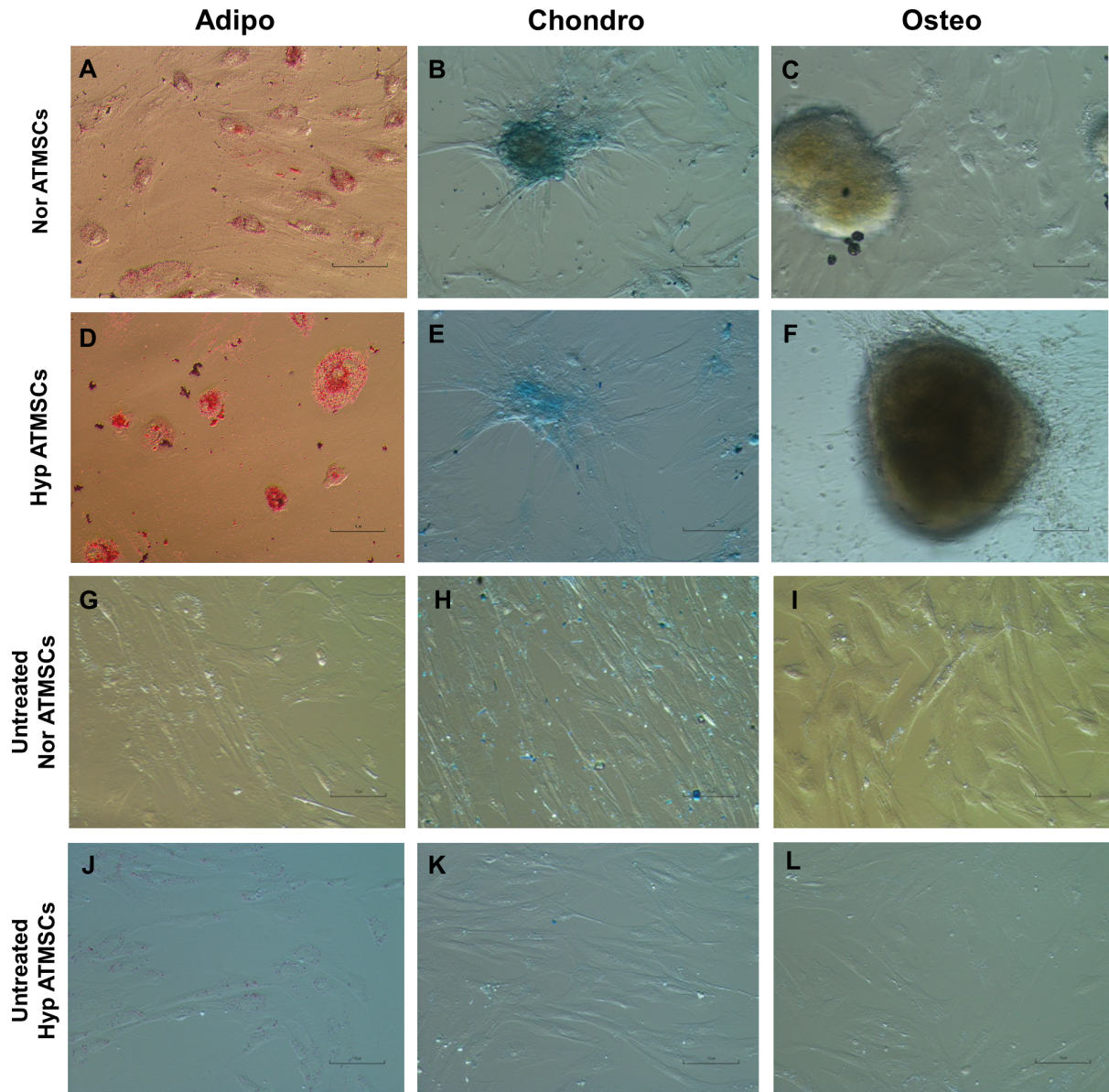




638 **Fig. 3.** A: Representative RT-PCR analysis of gene expression in canine AT-MSCs cultured  
639 in different oxygen atmospheres. CD44, CD34 expression was evaluated on samples at P3  
640 whereas dog leukocytes antigens expression was studied both at P0 and at P3. B: Flow  
641 cytometric analysis. Nor-AT-MSCs and Hyp-AT-MSCs samples analyzed for different  
642 antigens expression (CD90, CD105, CD14, CD45) by FACS analysis.

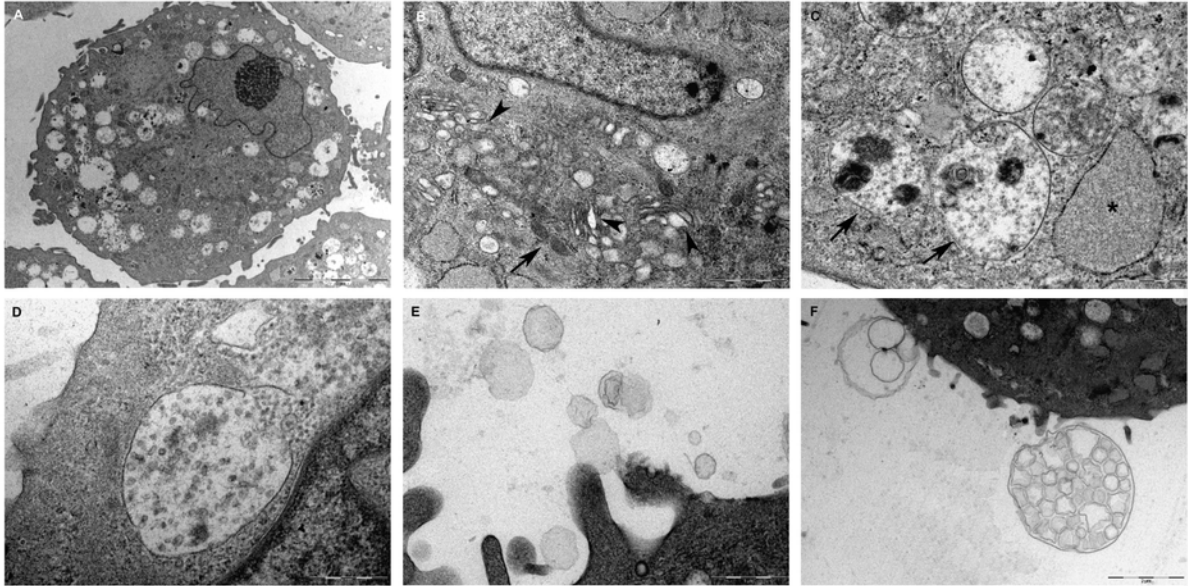


644 **Fig. 4.** Differentiation potential: Canine AT-MSCs cultured under adipogenic (A, D),  
 645 chondrogenic (B, E) and osteogenic (C, F) medium in normoxic and hypoxic conditions  
 646 respectively. G-L: Stained cells cultured in control medium. Magnification: 20X.

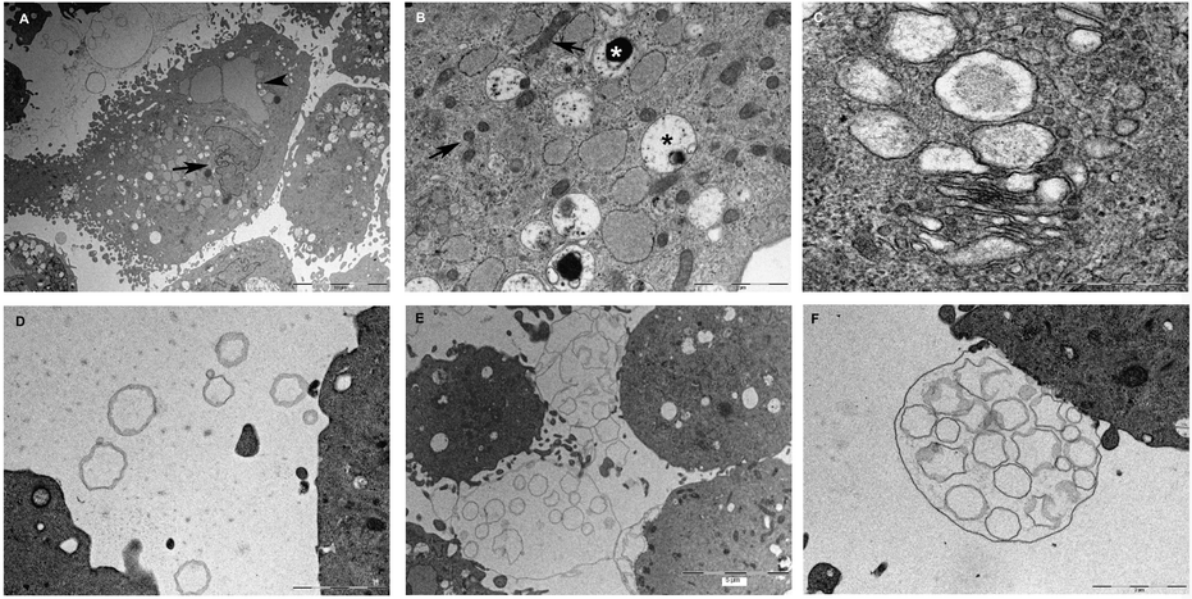


647  
 648 **Fig. 5.** Nor-AT-MSCs at TEM. **A.** At low magnification a single euchromatic irregular  
 649 nucleus containing a prominent nucleolus can be seen. Scale bar, 5 $\mu$ m. **B.** Note the abundance  
 650 of elongated mitochondria (arrow) and the well developed Golgi apparatus (arrowheads).  
 651 Scale bar 1  $\mu$ m. **C.** A group of endolysosomes with heterogeneous content can be observed  
 652 (arrows). Near them, a dilated RER cistern has been marked with an asterisk. Scale bar, 1 $\mu$ m.

653 **D.** A maturing MVB containing numerous endo-luminal vesicles. Scale bar, 500 nm. **E.**  
654 Numerous vesicles of heterogeneous size can be observed in the extracellular space. Scale  
655 bar, 1  $\mu\text{m}$ . **F.** Large complex electron-lucent vesicles budding from the cell surface and  
656 containing smaller vesicles. Scale bar, 2  $\mu\text{m}$ .



657  
658 **Fig. 6.** Hyp-AT-MSCs at TEM. **A.** Low magnification image showing a single euchromatic  
659 nucleus (arrow) and cytoplasm containing a prominent RER with dilated cisternae  
660 (arrowheads). Note the irregular cell profile determined by the presence of cytoplasmic  
661 pseudopodial evaginations. Scale bar, 10  $\mu\text{m}$ . **B.** Cell cytoplasm with abundant mitochondria  
662 (arrows), dilated RER and numerous MVB and endolysosomes (asterisks). Scale bar, 2  $\mu\text{m}$ .  
663 **C.** Golgi apparatus is wide and well developed and is characterized by flattened cisternae,  
664 transport vesicles, and large vacuoles, often filled with fine granular material. Scale bar, 500  
665 nm. **D.** The image shows the presence of vesicles of heterogeneous dimensions located in the  
666 extracellular space. Scale bar, 2  $\mu\text{m}$ . **E, F.** Note the presence of large vesicles shedding from  
667 the cell surface and containing round-shaped smaller vesicles inside their lumen. Scale bar, 5  
668  $\mu\text{m}$  and 2  $\mu\text{m}$ .



669

670

671 **Table 1:** Specific induction media compositions.

Adipogenic medium	Chondrogenic Medium	Osteogenic Medium
- DMEM/TCM199 - 10% FBS - 0.5 mM IBMX (removed after 3 days) - 1 $\mu$ M DXM (removed after 6 days) - 10 $\mu$ g/ml insulin - 0.1 mM indomethacin	- DMEM/TCM199 - 1% FBS - 6.25 $\mu$ g/ml insulin - 50 nM AA2P - 0.1 $\mu$ M DXM -10 ng/ml hTGF- $\beta$ 1	- DMEM/TCM199 - 10% FBS - 50 $\mu$ M AA2P - 0.1 $\mu$ M DXM - 10 mM BGP

672 IBMX: isobutylmethylxanthine, DXM: Dexamethasone, hTGF: human Transforming Growth

673 Factor, AA2P: Ascorbic Acid 2-Phosphate, BGP: Beta-Glycerophosphate

674

675 **Table 2:** Sequences of primers used for RT-PCR analysis

Gene	Primer sequences FW and RV	Amplicon (bp)	Reference
GAPDH	FW 5'- GGTCACCAGGGCTGCTTT -3' RV 5'- ATTTGATGTTGGCGGGAT -3'	209	(Jung et al. 2009)
CD44	FW 5'- GCCCTGAGCGTGGGCTTTGA -3' RV 5'-TCTGGCTGTAGCGGGTGCCA -3'	268	(Filioli Uranio et al. 2011)
CD34	FW 5'- GCCTGCTCAGTCTGCTGCCC-3' RV 5'- TGGTCCCAGGCGTTAGGGTGA -3'	255	(Filioli Uranio et al. 2011)
DLA-DRA1	FW 5'-CGCTCCAACCACACCCCGAA -3' RV 5'- GGCTGAGGGCAGGAAGGGGA-3'	246	(Filioli Uranio et al. 2011)
DLA-DQA1	FW 5'-GCACTGGGGCCTGGATGAGC -3' RV 5'-ACCTGAGCGCAGGCCTTGGA -3'	163	(Filioli Uranio et al. 2011)

676

677

678 **Table 3.** Primary antibodies and Isotype used for flow cytometry.

Markers	Ig
CD90 - PC5	IgG1
CD105 - PE	IgG2a
CD14 - PC5	IgG2a
CD45 - APC	IgG1
Isotype	
Isotype PC5	IgG2a
Isotype FITC	IgG1
Isotype PE	IgG1
Isotype APC	IgG1

679 Ig: immunoglobulin

680